CFD study on the effects of viscous shear in a hot cascade Ranque-Hilsch vortex tube

Nilotpala Bej[1] **and K P Sinhamahapatra**[1]

Wind Tunnel Lab, Department of Aerospace Engineering,
Indian Institute of Technology, Kharagpur, 721302, India

E-mail: nilotpala2002@gmail.com

Abstract. The objective of this paper is to carry out an extensive Computational Fluid Dynamics (CFD) study on work transfer due to viscous shear in a hot cascade Ranque -Hilsch vortex tube. The commercial CFD code ANSYS FLUENT 14.0 has been employed to carry out the numerical analysis using RANS standard k-epsilon turbulence model. A two-dimensional axisymmetric geometrical domain has been generated with structured mesh and air has been taken as the working fluid. The CFD results reveal that work transfer due to the action of viscous shear along the tangential direction increases considerably with hot cascading. However, the work transfer due to viscous shear along the axial direction degrades the performance of the device as the heat transfer takes place from cold zone to the hot zone. The effect of radial shear stress is negligible due to low value of radial velocity gradient.

1. Introduction

Ranque -Hilsch vortex tube is a device that is capable of splitting the highly compressed inlet gas into two streams of lower pressure gases, namely, central zone of cold fluid and peripheral zone of hot fluid around the inner wall of the tube. The thermal separation in a vortex tube depends on several geometrical and operational parameters and the process of thermal separation is still a topic of research as no theories explained it successfully. However, the work transfer due to viscous shear is considered to be the most widely acceptable theory proposed by (Hilsch, 1947) and subsequently supported by (Fröhlingsdorf and Unger, 1999, Colgate and Buchler, 2000, Aljuwayhel et al., 2005, Behera et al., 2008).

Though the vortex tube is basically used for cooling purposes, the hot gas can also be used for heating purposes to make efficient use of both the cold and hot gases produced by the device. However, the heating effect generated in a single stage vortex tube is not high enough which can further be used to achieve any useful work. Therefore, the method of hot cascading is an endeavor to make use of the cold gas for cooling purposes while improving the heating capacity of the hot gas, thereby enhancing the overall efficiency of the whole system. Exergy analysis based on experimental (Dincer et al., 2011) and numerical (Bej and Sinhamahapatra, 2014) studies confirm that efficiency of the device improves with hot cascading. The advantages of multiple staging over single stage vortex tube have been successfully reported in (Dincer, 2011, Guillaume and Jolly, 2001).

[1]Nilotpala Bej, E-mail: nilotpala2002@gmail.com

Content from this work may be used under the terms of the Creative Commons Attribution 3.0 licence. Any further distribution of this work must maintain attribution to the author(s) and the title of the work, journal citation and DOI.
Published under licence by IOP Publishing Ltd

2. Hot cascade arrangement and geometrical domain

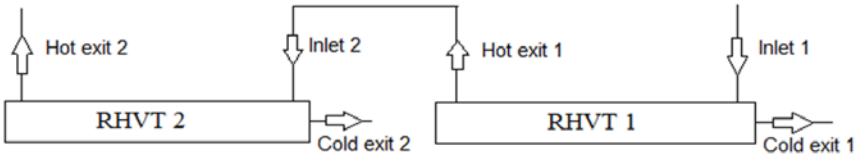

Figure 1: Schematic diagram of the hot cascade Ranque-Hilsch Vortex Tube

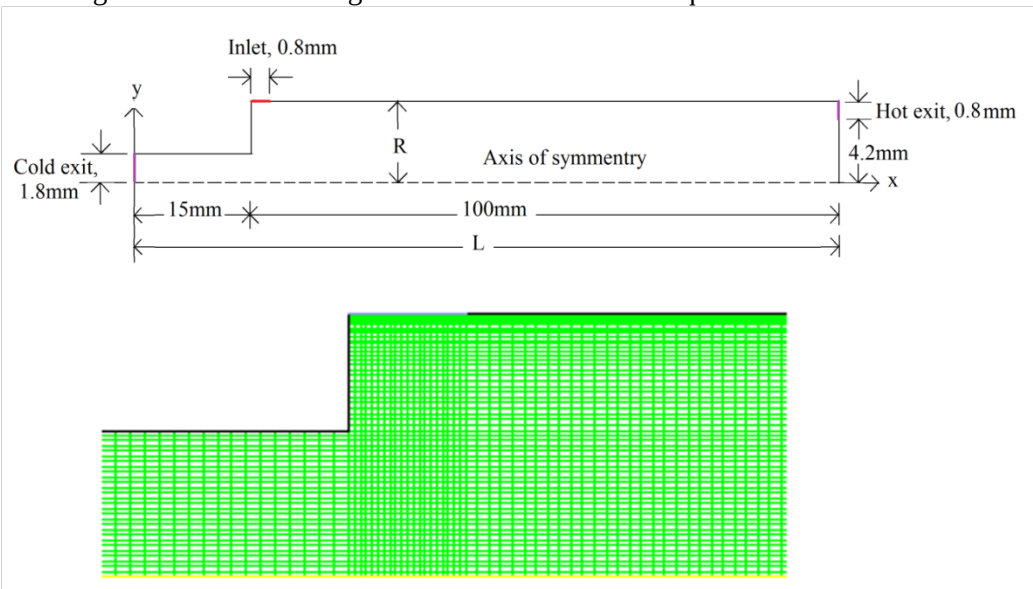

Figure 2: Geometrical domain of the second stage RHVT

In a hot cascade arrangement, there are two vortex tubes connected in series in such a way that the hot gas produced by the first stage of vortex tube serves as the inlet fluid for the second stage vortex tube. A schematic presentation of the hot cascade Ranque-Hilsch vortex tube is shown in figure 1. The geometrical domains of both the first and second stage vortex tubes are similar. A two-dimensional axisymmetric model of the vortex tube is generated with near wall refined mesh as shown in figure 2. However, as this paper is based on the study of effects of viscous shear due to hot cascading, therefore, prime attention is focused on the second stage vortex tube. The validity of the numerical model is evaluated through an overall temperature separation against the experimental data available in literature (Behera et al., 2005)

3. CFD model and Boundary conditions

The standard *k*-ε turbulent model in conjunction with continuity, gas state equation and Reynolds-averaged Navier–Stokes equations are employed to study the turbulent flow in the tube. The equations involved for turbulence energy and turbulence dissipation rate with standard notations are as follows:

$$\frac{\partial}{\partial x_i}(\rho k u_i) = \frac{\partial}{\partial x_j}\left[\left(\mu + \frac{\mu_t}{\sigma_k}\right)\frac{\partial k}{\partial x_j}\right] + P_k + P_b - \rho\varepsilon - Y_M + S_k \quad (1)$$

$$\frac{\partial}{\partial x_i}(\rho \varepsilon u_i) = \frac{\partial}{\partial x_j}\left[\left(\mu + \frac{\mu_t}{\sigma_\varepsilon}\right)\frac{\partial \varepsilon}{\partial x_j}\right] + C_{1\varepsilon}\frac{\varepsilon}{k}(P_k + C_{3\varepsilon}P_b) - C_{2\varepsilon\rho}\frac{\varepsilon^2}{k} + S_\varepsilon \quad (2)$$

The associated model constants are:
$Pr_t = 0.85$, $C_{1\varepsilon} = 1.44$, $C_{2\varepsilon} = 1.92$, $C_{3\varepsilon} = -0.33$, $C_\mu = 0.09$, $\sigma_\varepsilon = 1.0$, $Pr_t = 1.3$

The mass flow rate at the inlet of the second stage RHVT is fixed at 50% of the first stage RHVT. The boundary conditions applied for first and second stage RHVT are derived from the experimental work by (Dincer et al., 2011). Adiabatic and no slip conditions are set at all the solid walls. Total pressure at the inlet of first RHVT is fixed at 730kPa (abs). The static pressure at the cold exit of both tubes is set at 100kPa (abs). Zero temperature gradient is applied at both the hot and cold exits of both the vortex tubes. The first stage RHVT produces cold fraction value of 0.5 when the hot exit pressure is fixed at 440kPa. Therefore, inlet pressure of the second stage RHVT is fixed at 440kPa (abs). The hot exit pressures are varied to get the different values of cold fraction in second stage RHVT.

4. Mathematical formulation for work transfer due to viscous shear

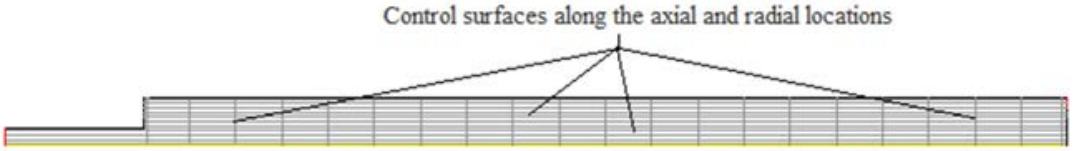

Figure 3: Control surfaces created for calculation of work transfer

To calculate the radial distribution of work transfer due to viscous shear, a numbers of control surfaces normal to the axis at different axial locations are considered. The first surface is created near the inlet (*x/L* = 0.13) and the last is close to hot exit (*x/L* = 0.98). Apart from these two, 19 more equidistant surfaces are created within the span of *x/L* = 0.13 to 0.98 as shown in figure 3. Similarly a number of control surfaces parallel to the axis of the vortex tube are created at the radial locations of *r* = 0.1mm,between 0.5mm to 4.5mm with an interval of 0.5mm and one at very close to the wall at *r* = 4.9mm.

a) Radial distribution of the rate of work transfer due to the viscous shear across a differential length of the control surface (*dr*):

The rate of tangential viscous shear work per unit length is calculated as follows

$$\frac{\delta \dot{W}_\theta}{dr} = -2\pi r \mu_{eff} w \frac{\partial w}{\partial x} \quad (3)$$

Where *x* is the axial co-ordinate and *w* is the swirl velocity (ms^{-1}).

Effective viscosity, $\mu_{eff} = \mu + \mu_t$

Similarly, rate of radial viscous shear work per unit length,

$$\frac{\delta \dot{W}_r}{dr} = -2\pi r \mu_{eff} v \frac{\partial v}{\partial x} \quad (4)$$

Where *v* is the radial velocity (ms^{-1}).

b) Axial distribution of the rate of work transfer due to the viscous shear across a differential length of the control surface (*dx*):

The rate of tangential viscous shear work per unit length

$$\frac{\delta \dot{W}_\theta}{dx} = -2\pi r \mu_{eff} w \left(\frac{\partial w}{\partial r} - \frac{w}{r}\right) \quad (5)$$

Rate of axial viscous shear work per unit length,

$$\frac{\delta \dot{W}_x}{dx} = -2\pi r \mu_{eff} u \frac{\partial u}{\partial r} \quad (6)$$

5. Results

5.1. Fluid flow study

The CFD study has been carried out to understand the fluid flows, namely velocity contours, pressure contours, behavior of streamlines and total temperature separation contours. Figure 4 represents the behavior of swirl, axial and radial velocity components along the radial distance from the axis when the cold fraction is fixed at 0.5. The magnitude of all the three components seems to reduce gradually

on moving towards the hot exit. The swirl velocity component has the highest value and positive throughout the vortex tube. However, the axial velocity component reverses its direction near the axis, and responsible for cold fluid to be generated at the opposite end of the hot exit. Though the trend of all there velocity components obtained from second stage RHVT remain similar to that of first stage RHVT, the magnitudes are found to be higher for same value of cold fraction.

The streamlines and temperature separation contours are shown in figure 5 and 6 respectively. It demonstrates that the axial heat transfer has degrading effects on the performance of the vortex tube within the region of cold exit and inlet. It implies that the flow in the middle and outer part of the cold exit zone has a tendency of gaining heat along the axial direction. Within the extended cold exit region the flow pressure and temperature rise along the outward radial that leads to gain in thermal energy.

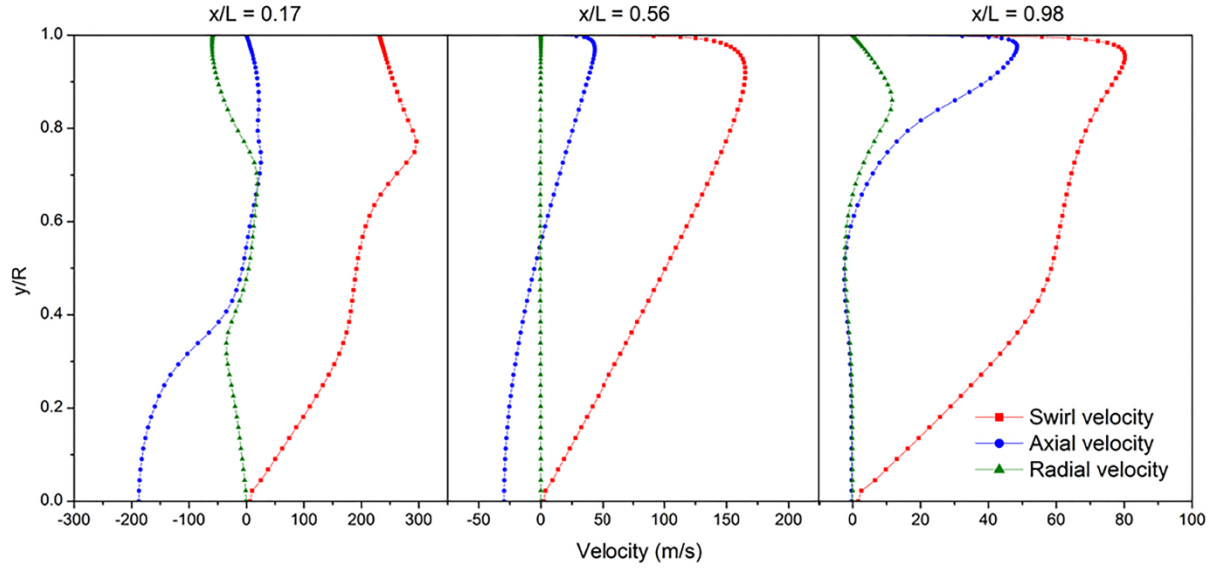

Figure 4: Radial distribution of swirl, axial and radial velocity components at the axial locations of *x/L* = 0.17, 0.56, and 0.98

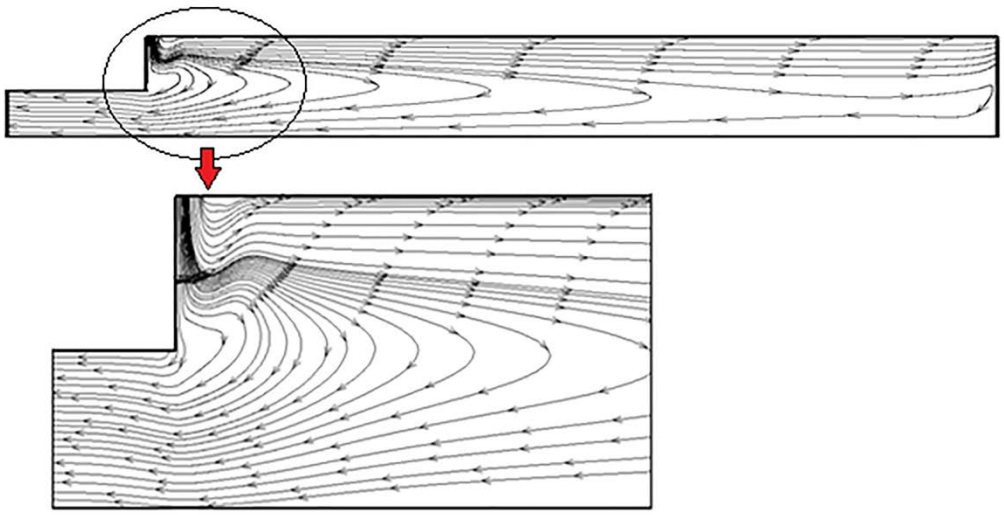

Figure 5: Streamline plots

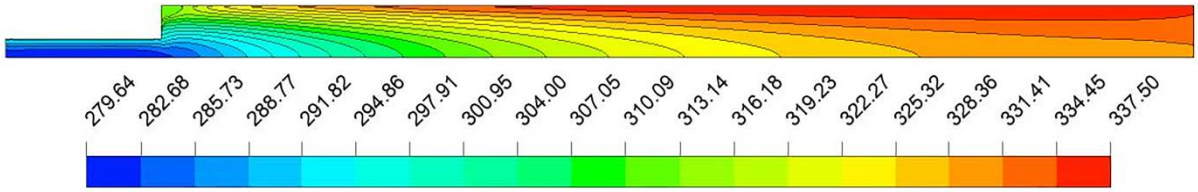

Figure 6: Total temperature contours

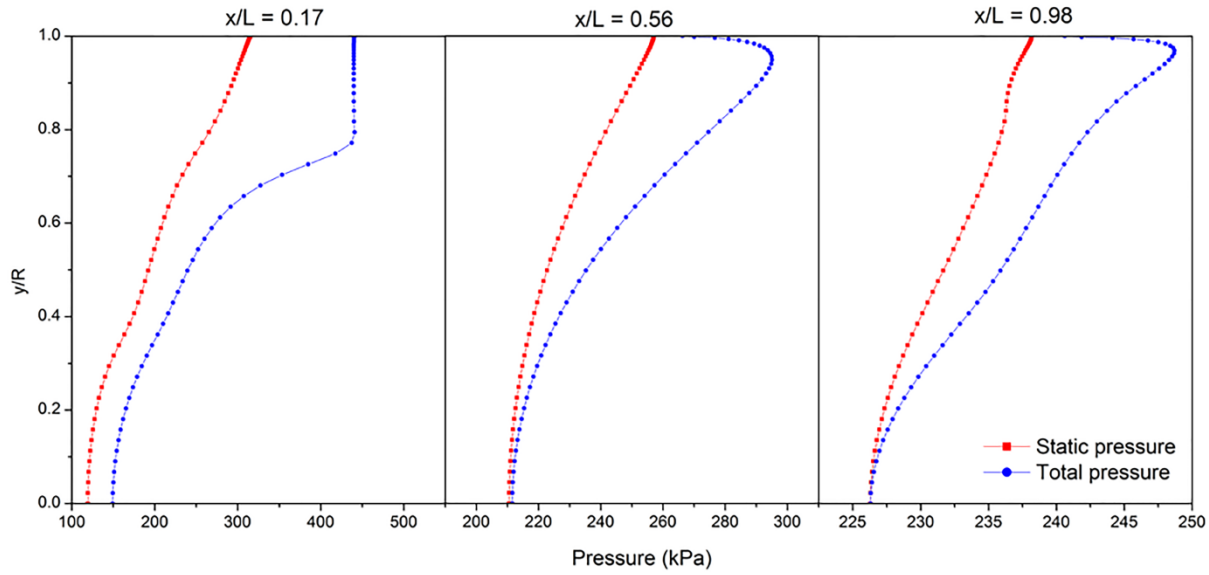

Figure 7: Radial distribution of static and total pressure at the axial locations of *x/L* = 0.17, 0.56, and 0.98

The radial distribution of total pressure and static pressure is shown in figure 7. The total pressure behaves similar to the swirl velocity component. It demonstrates that the total pressure gradient is mainly affected by the swirl velocity. However, the fluid moving towards the hot end is imposed by the drag force produced as a result of pressure gradient between the flow field and cold exit. The flow reversal happens when the fluid has no more momentum to flow against the pressure gradient. The fluid expands even after flow reversal till it reaches the atmospheric pressure at the cold exit. During the reversal of flow the difference in total pressure and static pressure values near the axis is found to be small. This pressure difference increases towards the wall of the vortex tube due to the increase in axial as well as swirl velocity.

5.2. Radial distribution of tangential and radial viscous shear work

The rates of work transfer in second stage vortex tube due to tangential and radial viscous shear are calculated using equation (3) and (4) respectively. Figure 8 represents the radial distribution of work transfer per unit length due to tangential and radial viscous shear at three axial locations, namely *x/L* = 0.17, 0.56 and 0.98when the cold fraction is 0.5. The process of tangential shear work transfer from the cold to hot fluid near the axis in this region can be attributed to very large pressure gradient near the inlet leading to intense turbulence. Turbulence drives the momentum from fluid near the axis towards the fluid around the vortex tube wall. Hence, the transfer of work due to tangential shear takes place from the cold zone to the hot zone. The profiles of tangential shear work transfer start with zero at the axis, then become positive and remain so until *y/R* = 0.8 and finally changes to negative as they approach the vortex tube wall. The effects of work transfer due to radial shear at the axial locations are also shown in figure 8. The magnitudes are too small due to low values of radial velocity

gradients. Therefore, the effect of radial shear work on the thermal separation is practically negligible and can be ignored in the study of vortex tube performance.

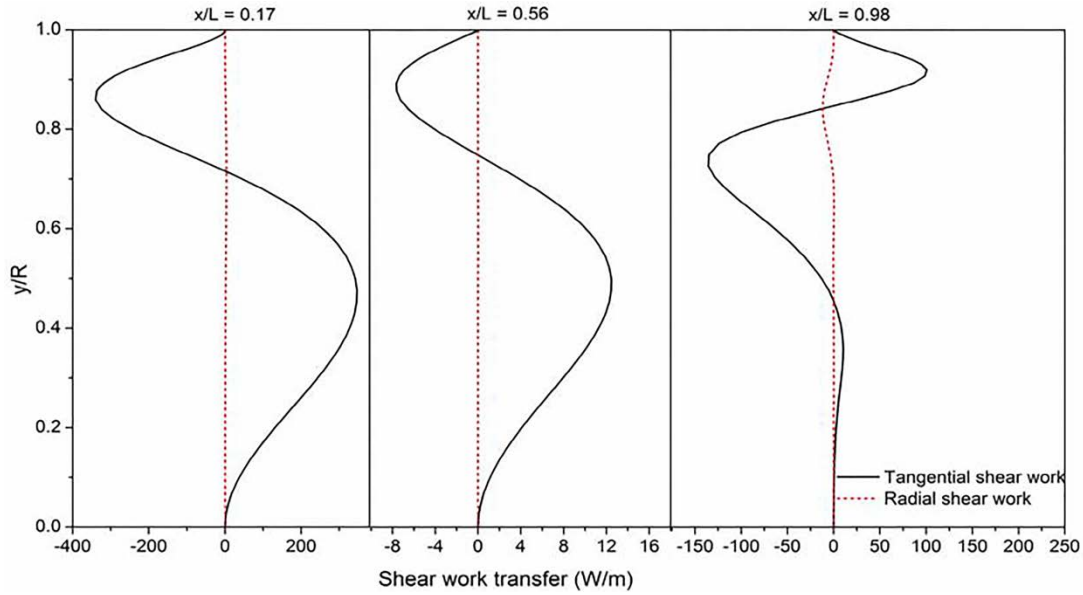

Figure 8: Radial distribution of tangential and radial viscous shear work transfer per unit length at the axial locations of x/L = 0.17, 0.56, and 0.98

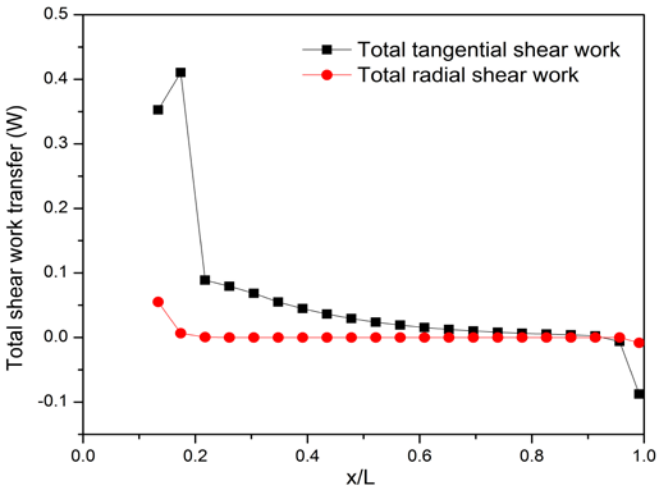

Figure 9: Radial distribution of total tangential and radial viscous shear work transfer

5.3. Total tangential and radial viscous shear work transfer across the radial surfaces

The total work transfer due to tangential and radial shear work for the respective control surfaces are calculated by integrating equations (3) and (4) over the whole control surface. Figure 9 shows radial distribution of total tangential and radial viscous shear work transfer at the axial locations of x/L = 0.17, 0.56 and0.98 when cold fraction is 0.5. Though the work transfer is found positive throughout the length of the vortex tube, the magnitude is too small. So, it can be concluded that the contribution of work transfer due to radial distribution of tangential and radial shear work in the process the temperature separation in second stage vortex tube is negligible.

5.4. Axial distribution of tangential and axial viscous shear work

The axial distribution of work transfer per unit length due to the tangential and axial viscous shear at the radial locations of y/R = 0.1, 0.5 and 0.99 is analyzed in figure 10. The tangential shear work is found to be positive over all the control surfaces, whereas the axial shear work is observed to be negative for y/R = 0.99 i.e. the surface near the vortex tube wall. The work transfer due to tangential viscous shear has a very high value as compared to that due to axial viscous shear. However, the value of both the work transfer reduces vigorously beyond the length of x/L = 0.4 to 0.5 depending on the value of y/R. This can be interpreted as the stagnation region within which maximum temperature separation occurs. It is also noted that maximum work transfer occurs near the inlet due to higher pressure gradient in this region.

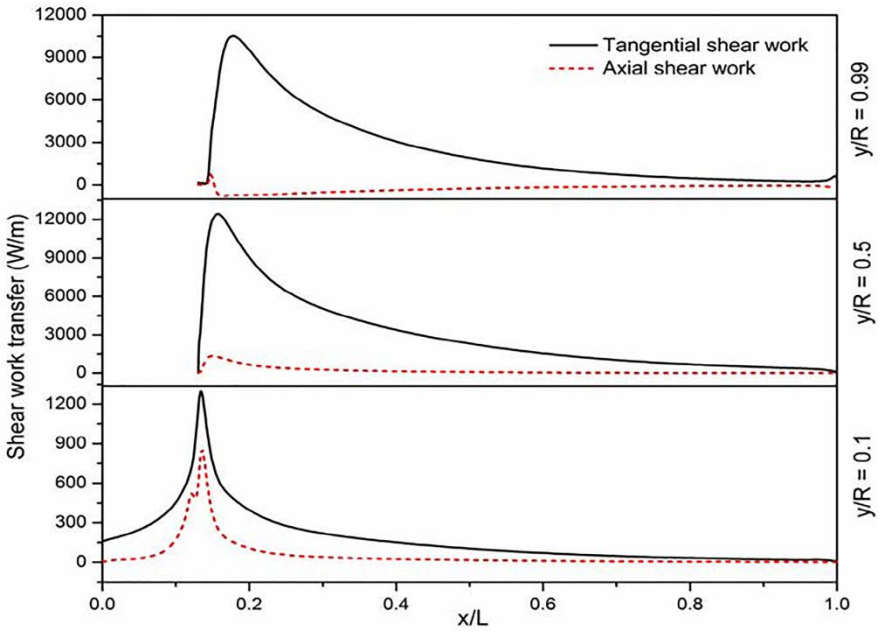

Figure 10: Axial distribution of tangential and axial viscous shear work transfer per unit length at the radial locations of y/R = 0.1, 0.5, and 0.99

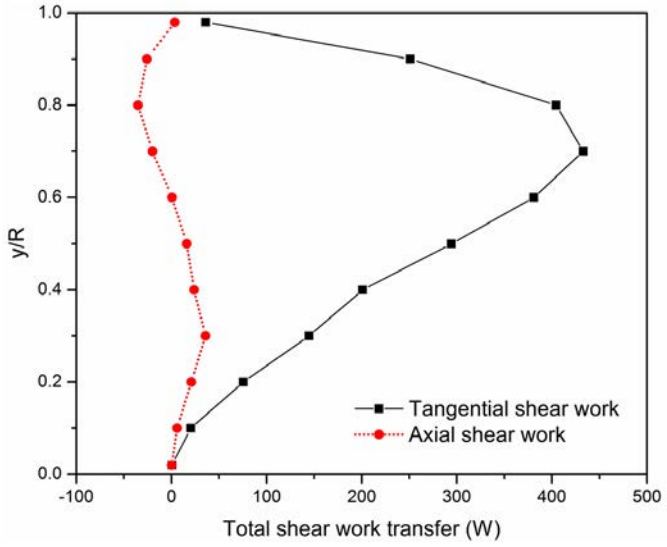

Figure 11: Axial distribution of total tangential and axial viscous shear work transfer

5.5. Total tangential and axial viscous shear work transfer across the axial surfaces

The total tangential and axial viscous shear work transfer is calculated using equation (5) and (6) integrated over the whole control surface. Figure 11 depicts the comparison study of axial distribution of total work transfer due to tangential and axial viscous shear. It is very clear from the figure that tangential shear work plays the utmost role in the process of thermal separation. However, the net work transfer at a particular point in the vortex tube is the resultant of work transfer, both axial and radial distribution of tangential, axial, and radial viscous shear.

6. Conclusions

Maximum work transfer due to tangential shear occurs near the inlet where maximum expansion of the gas takes place. This confirms that the tangential shear drives the energy from cold fluid zone to hot fluid zone as a result of pressure drop. The profiles of work transfer due to tangential and axial viscous shear show that the difference of work transfer between the peripheral to central core zones decreases on moving towards the hot exit. Maximum temperature separation occurs within an axial span of x/L = 0.17 to 0.50 and radial span of y/R = 0.40 to 0.60. That the action of viscous shear on fluid layers improves the conversion of kinetic energy into thermal energy has been confirmed. Thermal separation in second stage vortex tube of hot cascade type RHVT takes place mainly along the axial direction due to the effects of tangential and axial viscous shear work transfer.

References

[1] Aljuwayhel N F, Nellis G F and Klein S A 2005 Parametric and internal study of the vortex tube using a CFD model. *International Journal of Refrigeration,* **28,** 442-450

[2] Behera U, Paul P J, Dinesh K and Jacob S 2008 Numerical investigations on flow behaviour and energy separation in Ranque–Hilsch vortex tube. *International Journal of Heat and Mass Transfer,* **51,** 6077-6089

[3] Behera U, Paul P J, Kasthurirengan S, Karunanithi R, Ram S N, Dinesh K and Jacob S 2005 CFD analysis and experimental investigations towards optimizing the parameters of Ranque–Hilsch vortex tube. *International Journal of Heat and Mass Transfer,* **48,** 1961-1973

[4] Bej N and Sinhamahapatra K P 2014 Exergy analysis of a hot cascade type Ranque-Hilsch vortex tube using turbulence model. *International Journal of Refrigeration,* **45,** 13-24

[5] COLGATE S A and BUCHLER J R 2000 Coherent transport of angular momentum. The Ranque-Hilsch tube as a paradigm. *Ann. New York Acad. Sci.,* **898,** 105-112

[6] Dincer K 2011 Experimental investigation of the effects of threefold type Ranque–Hilsch vortex tube and six cascade type Ranque–Hilsch vortex tube on the performance of counter flow Ranque–Hilsch vortex tubes. *International Journal of Refrigeration,* **34,** 1366-1371

[7] Dincer K, Yilmaz Y, Berber A and Baskaya S 2011 Experimental investigation of performance of hot cascade type Ranque–Hilsch vortex tube and exergy analysis. *International Journal of Refrigeration,* **34,** 1117-1124

[8] Fröhlingsdorf W and Unger H 1999 Numerical investigations of the compressible flow and the energy separation in the Ranque-Hilsch vortex tube. *International Journal of Heat and Mass Transfer,* **42,** 415-422

[9] Guillaume D W and Jolly J L 2001 Demonstrating the achievement of lower temperatures with two-stage vortex tubes. *Review of Scientific Instruments,* 72**,** 3446-3448

[10] Hilsch R 1947 The use of the expansion of gases in a centrifugal field as cooling process. *Rev. Sci. Instrum,* **18,** 108-113